Spreading of Neutrophils: From Activation to Migration

Kheya Sengupta,*§ Helim Aranda-Espinoza,†¶ Lee Smith,‡ Paul Janmey,* and Daniel Hammer†‡
*Institute for Medicine and Engineering, †Department of Bioengineering, and ‡Chemical and Biomolecular Engineering, University of Pennsylvania, Philadelphia, Pennsylvania; and §Institut für Schichten und Grenzflächen–IV, Biologische Schichten, Forschungszentrum Jülich GmbH, D-52425 Jülich, Germany

ABSTRACT Neutrophils rely on rapid changes in morphology to ward off invaders. Time-resolved dynamics of spreading human neutrophils after activation by the chemoattractant fMLF (formyl methionyl leucyl phenylalanine) was observed by RICM (reflection interference contrast microscopy). An image-processing algorithm was developed to identify the changes in the overall cell shape and the zones of close contact with the substrate. We show that in the case of neutrophils, cell spreading immediately after exposure of fMLF is anisotropic and directional. The dependence of spreading area, A, of the cell as a function of time, t, shows several distinct regimes, each of which can be fitted as power laws ($A \sim t^b$). The different spreading regimes correspond to distinct values of the exponent b and are related to the adhesion state of the cell. Treatment with cytochalasin-B eliminated the anisotropy in the spreading.

INTRODUCTION

The adhesion of cells is crucial for the physiological processes of cell growth, motility, development, immune response, and wound healing. Because of their specific function as the body's first defense against infection or injury, neutrophils are required to be highly motile. Neutrophils reside in the blood stream and when presented with certain chemicals (chemoattractants) that are secreted in response to infection or injury they are activated. The process of activation triggers a cascade of events that lead to spreading and finally migration (1,2). Early in inflammation, neutrophils passively roll along the endothelial wall, and this rolling has been a subject of great interest both theoretically and experimentally (3–5). Soon afterwards, the neutrophil is activated and begins integrin-mediated spreading (6) and finally undergoes migration along the surface of endothelial cells or transmigration through the endothelium (7). Before migration, the cells polarize. They develop a distinct front or leading edge which is rich in filamentous actin and is called the lamellipodium and a back or trailing edge which is rich in actomyosin complexes and is called the uropod. Acquiring such a shape enables the cell to convert cytoskeletal chemical interactions into net cell-body displacements. The particular interest of this work is the role of adhesion in the initial spreading of neutrophils.

Because of the importance of cell spreading, there have been considerable experimental and theoretical efforts to quantify it. However, studies involving detailed analysis of the dynamics of cell spreading have been possible only recently, owing to the development of novel microscopic techniques, fast cameras, and rapid data analysis (8–13). Even a relatively simple system like red blood cells spreading passively on poly-lysine due to charge-induced attraction exhibits rather complex behavior (12). The complexity involved in adhesion of nucleated cells has been revealed in a series of recent experiments, including those by Dubin-Thaler et al. (8) where total internal reflection fluorescence (TIRF) microscopy was used to follow the spreading of fibroblasts on fibronectin, Reinhart-King et al. (9) where traction force microscopy (TFM) was used to measure the traction stresses of endothelial cells during spreading, and Zicha et al. (10) where fluorescence localization after bleaching was used to measure the transport of actin to protruding zones of rat fibroblasts. In a study systematically exploring the role of passive (self-assembly due to imposed physical forces) and active contributions to the spreading of monocytes, Pierres et al. (11) showed that initial cell surface alignment is driven by the interplay between adhesive forces and passive membrane deformations, but this process is accelerated by cytoskeleton-driven membrane motion.

Attempts have also been made to theoretically model cell spreading. Whereas the later stages of cell spreading are dominated by active processes involving signaling and stabilization by the cytoskeleton, the very early stage is expected to be dominated by self-assembly (13) and therefore is thought to be amenable to similar treatment as vesicle spreading. About a decade ago, Bell et al. (14,15) laid down the foundations of the theoretical framework to describe adhesion mediated by reversible bonds between cell surface molecules. This model, based on relatively simple thermodynamic arguments, has, over the years, been partially validated (11,12,16). In a similar spirit, Frisch et al. (17) attempted to describe the kinetics of spreading of fibroblasts on glutaraldehyde using the wetting theory of liquids. More recently, Chamaraux et al. (18) have included the biochemical process of actin polymerization in their model of a spreading amoeba, *Dictyostelium*

Submitted January 15, 2006, and accepted for publication July 27, 2006.

Address reprint requests to Kheya Sengupta, E-mail: k.sengupta@fz-juelich.de; or Daniel Hammer, E-mail: hammer@seas.upenn.edu.

Helim Aranda-Espinoza's present address is Dept. of Chemical and Biomolecular Engineering and Bioengineering Graduate Program, 2113 Bldg. 090, University of Maryland, College Park, MD 20742.

0006-3495/06/12/4638/11 $2.00

doi: 10.1529/biophysj.105.080382

discoideum. Both of these models predict a monotonic increase in cell area but with different growth laws. In neither model is there a distinction made between the total spread area of the cell and the area of the adhesive tight contacts.

An essential but poorly understood step that leads from activation to migration is the polarization of the cell. It has been known for some time that neutrophils migrate up a chemoattractant gradient (6,19,20). However, even when stimulated by an isotropic bath of the chemoattractant, neutrophils exhibit persistent polarization and migrate in randomly chosen directions. Concomitant with the obvious morphological polarization and actin accumulation at the leading edge, various other proteins as well as lipids (21) are preferentially sorted either to the lamellipodium (e.g., actin, PIP3, rac) or the uropod (e.g., actin-myosin complex, myosin II, Rho) (22,23). Since this remarkable asymmetry occurs even when the external chemotactic signal is uniform, it suggests that at least one signaling step leads to an internal polarization of the cell. Moreover, the chemoattractant receptors are typically distributed uniformly over the cell surface even after polarization (24), indicating that this internal signal occurs some time between receptor occupancy and actin polymerization. The exact point at which polarization occurs and the precise relationship between the biochemical and morphological polarization are not known.

Our study of the very early stages of neutrophil spreading focuses on the onset of polarity by observing morphological changes and the establishment of the first close contact with the substrate. Using RICM, we show that after the first exposure to a chemoattractant (either uniform or presented as a gradient) the cell is polarized even while it spreads. This anisotropic spreading pattern presages the ultimate direction of migration. We further show that there are distinct dynamics during neutrophil spreading characterized by different adhesion states as well as spreading rates. After activation there is an initial phase where spreading is slow, then spreading accelerates, typically after the apparition of zones of close contact with the substrate, and culminates in a fast phase of spreading which just precedes motility. Finally we discuss a possible mechanism that may be responsible for the observed behavior.

MATERIALS AND METHODS

Substrate

Glass coverslips (No. 1.5) were successively coated with fibronectin (or ICAM-1) and bovine serum albumin (BSA) (Sigma, St. Louis, MO) by incubating in 100 μg/ml solutions for ~20 min at room temperature. The coverslips were rinsed with PBS buffer after each coating step.

Neutrophil isolation and activation

Whole blood was taken from healthy donors into BD Vacutainers containing K_3EDTA (Becton Dickenson, Franklin Lakes, NJ). Seven milliliters of whole blood were layered onto 4 ml of dextran density gradient (Robbins Scientific, Sunnyvale, CA) and centrifuged at 500 $\times$ g for 60 min. The polymorphonuclear leukocytes (PMN) layer was washed once with Hanks' balanced salt solution (HBSS) (without Ca and Mg). The PMNs were counted and placed in HBSS (without Ca and Mg) + 0.1% human serum (Golden West Biologicals, Temecula, CA) + 10 mM HEPES (BioWhittaker, Walkersville, MD). Before the experiment, Ca^{2+} (1.5 mM) and Mg^{2+} (2 mM) were added to the PMNs and incubated at 37°C for 10 min. PMNs were transferred to a chamber with the fibronectin-coated coverslip and allowed to sediment. After sedimentation PMNs (neutrophils) were stimulated with formyl methionyl leucyl phenylalanine (fMLF, 2–10 nM).

Activation using a micropipette—creation of fMLF gradient

Borosilicate capillaries of 1-mm diameter (Friedrich & Dimmock, Millville, NJ) were pulled to form a micropipette with a small tip of 2–4-μm diameter. The micropipette was filled with HBSS (1.5 mM Ca^{2+} and 2 mM Mg^{2+}) + 0.1% human serum + 10 mM HEPES + 50 mM fMLF and mounted on a micromanipulator (Narishige, Tokyo, Japan). The micropipette was then positioned close to the selected neutrophils and the chemoattractant was continuously released, forming a chemoattractant gradient.

Actin depolymerization

Cells were incubated in 2 μM cytochalasin-B or latrunculin-A for 10 min. They were then transferred to the observation chamber and were activated by addition of fMLF.

Reflection interference contrast microscopy

Spreading was observed in reflection interference contrast microscopy (RICM) mode through an inverted microscope (Axiovert 200, Karl Zeiss, Goettingen, Germany) equipped with an antiflex 63$\times$ oil immersion (numerical aperture = 1.3) objective and appropriate polarizers. The sample was illuminated through the objective by a monochromatic light beam (wavelength: 546 nm) generated by passing the light from a 100-W mercury vapor lamp (Osram, Munich, Germany) through an interference filter (IF_g 546.1 nm, 85% transmission, 12-nm waveband). Images were recorded with a charge-coupled device camera (Retiga EXi Fast Cooled Mono 12-bit camera 32-0082B-128 QIMAGING, Burnaby, Canada). Typically, one frame was recorded per second and up to 1000 frames were saved for each cell-spreading event.

The principle of RICM and its application to quantitative analysis of dynamics of adhesion of vesicles and cells has been described before (25,26). In brief, monochromatic light is incident on the cell under study which hovers over a glass substrate in a transparent buffer. The incident light is reflected from the glass-buffer interface and again from the buffer-cell interface. These two reflected rays interfere and give rise to an interference pattern. When the two interfaces are very close together, that is, when the cell adheres to the substrate, the path difference between the interfering rays is zero and the interferrogram exhibits a minimum in the intensity. As the membrane curves away from the substrate, the path difference increases and the corresponding intensity on the interferrogram also increases. It passes through a maximum and starts to decrease again till finally the path difference is equal to half the wavelength of the light being used and the intensity is again a minimum. Thus, a pattern of alternating dark and bright fringes is obtained that reflects the height distribution of the lower surface of the cell membrane.

Typically, in RICM, the image of a cell has a patchy bright and dark appearance against a uniformly gray background. The dark zones correspond to areas where the membrane is close to the substrate. The closer the membrane is to the substrate, the darker the corresponding area is in the image. Therefore, the tightly adhered areas of the cell show up as dark patches in RICM. In Pierres et al. (11) it was shown that these patches represent tight adhesion inasmuch as the cells exhibiting dark patches do not roll or flow

with the fluid in a flow chamber. In Riveline et al. (27) it was shown that in the case of fibroblasts, the dark patches correspond to legitimate focal adhesions as revealed by immunostaining. In our analysis we make the reasonable assumption that the dark zones in RICM correspond to an area of intimate contact of the cell membrane with the substrate, in other words, tight adhesion.

DATA ANALYSIS

RICM

The surface of a quiescent neutrophil is rather rough (28) because of the presence of microvilli. Consequently, the alternating dark and bright fringes seen in RICM in the case of vesicles (25,29), red blood cells (12), or macrophages (11) are absent in the case of neutrophils. Instead, the light scattered from the numerous protrusions on the surface of the neutrophil results in an RICM pattern that looks like a uniformly bright disk against a gray background (Fig. 1 *A*). The bright-field image just after stimulation by fMLF looks grainy with a clearly defined outline (Fig. 1 *B*). However, unlike RICM images, no information about the height of the cell can be extracted from such an image. After activation, the neutrophil starts to spread (Fig. 1 *A*). The membrane area increases and the membrane is more clearly visible, indicating that it comes closer to the substrate. The cell now develops a bright and dark patchy appearance. A simple intensity threshold algorithm is not enough to identify the cell boundaries since it contains both brighter and darker than average intensities. A further complication arises from the fact that it is very difficult to get the background intensity across the field of view to be uniform (11). A novel algorithm, described below, was developed to simultaneously identify the boundaries of the cell and the adhesion zones inside the boundaries.

Algorithm to identify the cell

We exploit the fact that the intensity of the background is more uniform than the intensity of the cell, i.e., the spread in intensity of the background is narrower than the spread in intensity within the cell. This is true especially for the nonadherent parts of the cell. A similar idea forms the basis of the so-called variance filter frequently used in image processing. However, as described below, a simple variance filter is not sufficient in this case to identify the cell's spread area. Examples of typical intensity distribution for a pixel in the background in a nonadherent part of the cell and an adherent part of the cell are shown in Fig. 1, *C–F*. An algorithm (described below) is used to identify the pixels that correspond to the cell and assign a value of 2 to these pixels. All the other pixels are assigned the value 0. Thus a binary image of the cell is obtained. Next, the pixels corresponding to the dark tight adhesion (close contact) zones are identified and assigned the value 1. In this way, an image is obtained where three distinct regions, namely, the background, the cell body, and the dark adhesion zones, are clearly marked out in different colors. We shall refer to such images as trinary images.

The algorithm to get the binary (and trinary) image is as follows. First, a pixel is selected as the center of a 5×5 pixel matrix. The intensity histogram of the matrix is fitted with a Gaussian. The fitted parameters are the position of the center (which corresponds to the average intensity in each 5×5 box) and the width of the Gaussian (which corresponds to the spread in intensity within each box) for each pixel, which are stored in two matrices (each with dimensions equal to the original image), which we call the average-image and the width-image, respectively. From the width-image, a threshold for the width ($W_{\min}$) is determined by simple visual inspection such that all pixels in the width-image whose value is $<W_{\min}$ correspond to the background and the rest correspond to the cell. All pixels with value $<W_{\min}$ are assigned the

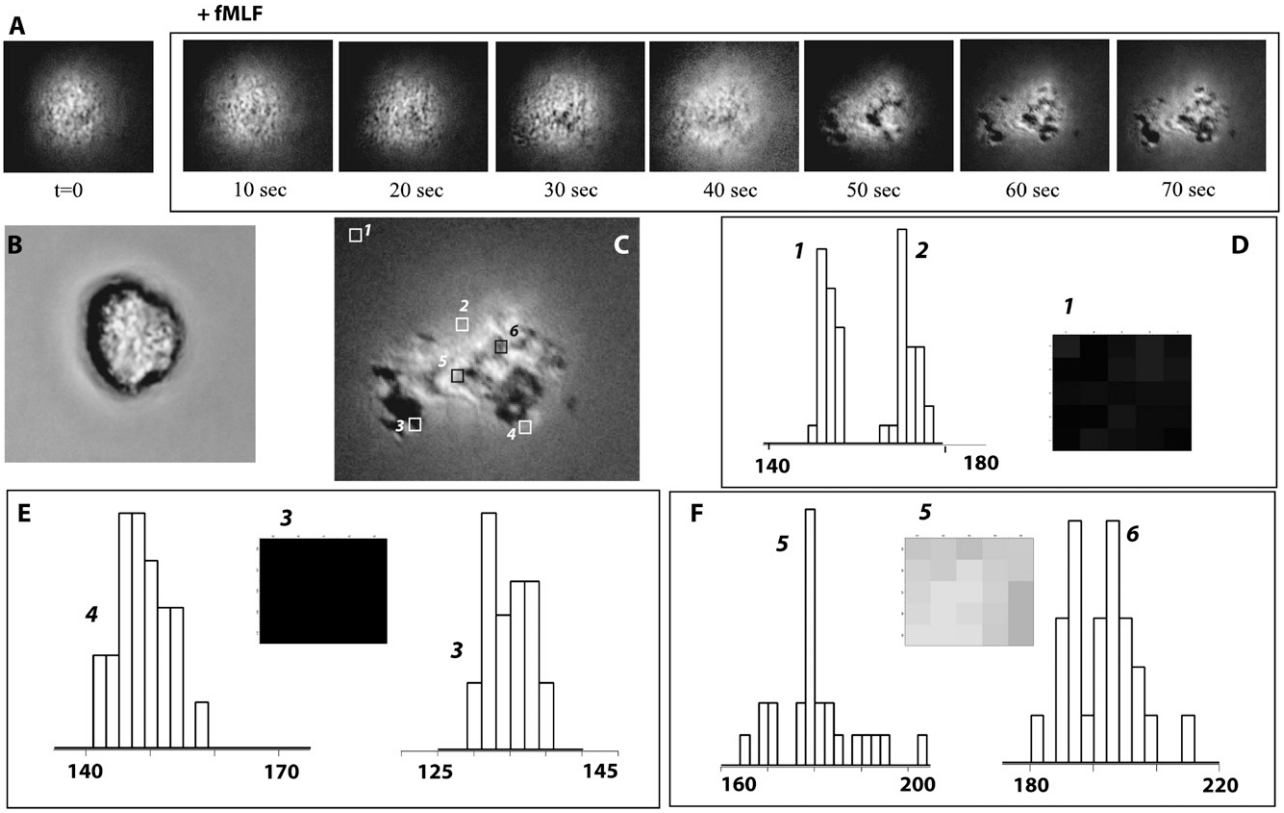

FIGURE 1 (*A*) Time-resolved RICM of early stages of neutrophil adhesion after activation by addition of fMLF into the bulk solution. Note that the cell shape begins to exhibit anisotropy before formation of close contact (*dark* in RICM) with the substrate. (*B*) Bright-field picture of a neutrophil just after addition of fMLF. (*C–F*) Image at 70 s indicating the positions of 5-pixel wide boxes and corresponding histograms of intensities. The boxes and the corresponding histograms are labeled with the same number.

value 0 and the rest are assigned the value 2. The validity of the value for W_{min} is checked by comparing with the original image.

However, by this procedure alone, the tightly adhering areas within the cell (that appear as uniformly dark) frequently are incorrectly assigned to the background. To correct for this, a threshold for the averaged intensity (I_{min}) is determined from the average-image in such a way that all pixels with values $>I_{min}$ correspond to either the background or to the bright area within the cell. I_{min} is usually the intensity of the darkest pixel in the background. In case there is an ambiguity in determining I_{min} in this way, it is determined by the following procedure: First a histogram of the entire average-image is made. When there are dark adhesion zones present in the image, in addition to the large peak corresponding to the background intensity, a small second peak appears in the histogram which corresponds to these dark zones (Fig. 2 *A*). A Gaussian of width σ is fitted to the second peak, and I_{min} is then equal to the peak intensity of this second peak minus σ. All the pixels with value $<I_{min}$ are identified as being within the cell and are reassigned the value 2. A new binary image of the cell is thus created where the pixels corresponding to the cell are all assigned the value 2 and the pixels corresponding to the background are assigned the value 0. Now, to create the trinary image, the pixels with average intensity value $<I_{min}$ are again identified as tight adhesion zones and are assigned the value 1 and the rest are assigned the value 0. An overlay with the binary image yields the trinary image. Fig. 2 *B* illustrates the various transformations the image undergoes.

Automating the procedure

The recorded digital images corresponding to one complete cell-spreading event are loaded into commercially available data analysis software (Igor Pro from WaveMatrix, Portland, OR). The first frame, where the cell typically is not spread at all, is considered. The threshold value of W_{min} is determined from the corresponding width-image by the procedure described above. Next, the last frame, where the cell is typically spread and exhibits dark adhesion zones, is considered. The threshold value of I_{min} is determined from the corresponding average-image by the procedure described above. When satisfactory binary image and trinary images are obtained for the first frame and last frame, the same values for W_{min} and I_{min} are used on all the other frames to obtain the corresponding binary and trinary images. From the binary images, all the parameters reported below can be determined by standard procedures; for example, the cell profile is determined by using a simple edge-detection algorithm incorporated into our customized Igor procedures.

RESULTS

Spreading initiation, first contact, and growth curves

Initially, the quiescent neutrophils sediment down and hover at a height of around 100–200 nm over the glass surface and show up in RICM as faint bright disks. When fMLF is added (either as a uniform concentration or through a micropipette providing a gradient), they are activated within seconds and start spreading. The cell area grows monotonically and finally reaches an asymptotic saturation value. Often, when the cell starts to migrate, the cell area oscillates around this final value.

A typical plot of the boundaries of a spreading cell (Fig. 3, *A* and *B*) reveals that the cell does not spread isotropically; it spreads preferentially in a particular direction so that one edge of the membrane seems to be ''pinned'' (indicated in Fig. 3, *A* and *B*, as a *curved arrow* bracketing the pinned edge). This

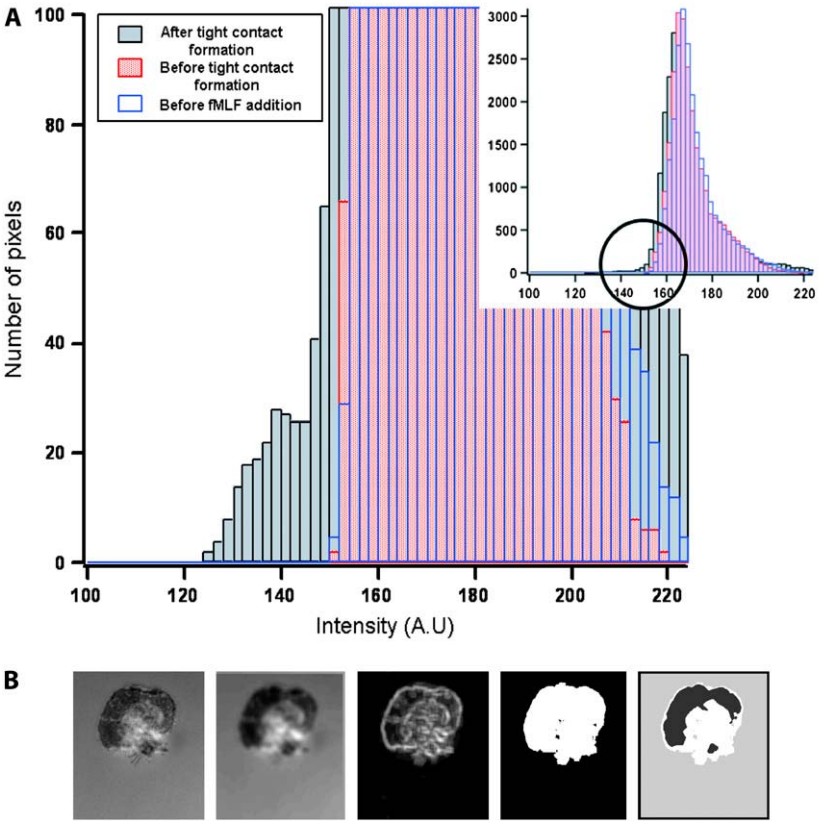

FIGURE 2 (*A*) Histogram of intensity distribution on entire images of a cell in the initial (before addition of fMLF), intermediate (before tight contact formation), and late (after tight contact formation) stages of spreading. The inset shows the entire histogram, and the main image is a zoom in on the low intensity part. The total number of pixels remains constant from image to image; however, the distribution of intensity changes. The large peak at intermediate intensities in the inset corresponds to the intensity of the background since most of the pixels in the image have that intensity. When ''tight contact'' forms, pixels that were previously bright (or intermediate) become considerably darker, resulting in the appearance of a small peak at low intensities which is apparent in the main image. (*B*) A spreading cell; (*from left to right*) raw RICM image, average-image, width-image, binary image, and trinary image. See text for explanation.

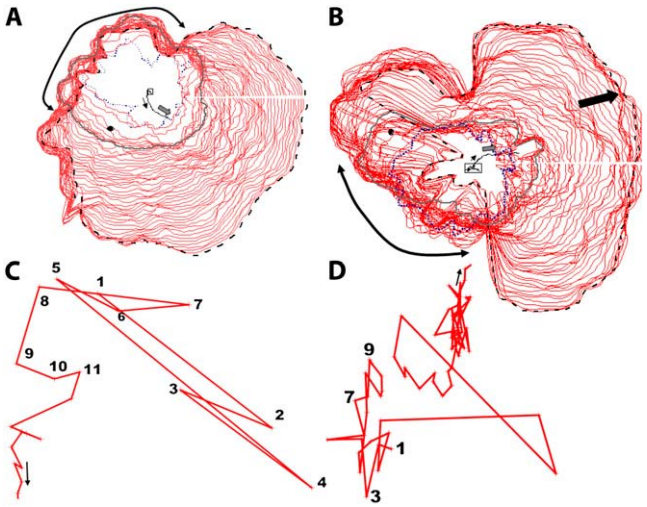

FIGURE 3 (*A* and *B*) The boundaries of a cell as it spreads after activation by either addition of fMLF into the bulk (*A*) or by presentation of a gradient in fMLF (*B*). The red closed lines represent cell boundary profiles separated in time by either 2 s (*A*) or 4 s (*B*). The direction of the fMLF gradient is shown as a thick black arrow in the right-hand corner of *B*. Note that as the cell spreads, one edge of the contour hardly moves (indicated by *curved arrows* bracketing the pinned zone). The trajectory of the centroid is shown as a thin black line inside the cell boundaries. The shape of the cell boundary just after addition of fMLF is shown as a blue dotted line, the shape just before beginning of migration as a broken black line, and the shape corresponding to the appearance of the first point of close persistent contact with the substrate as a solid gray line. In both cases, the approximate position of the first point of contact is indicated by a black filled oval, and the eventual direction of migration as a gray filled arrow next to the trajectory of the centroid. Note that in the case of uniform stimulation, the first point of close contact is roughly in the zone that later becomes the lamellipod, whereas in the case of a gradient in the concentration of fMLF, the first point of contact is in a zone that later becomes the uropod. (*C* and *D*) Close-up of the trajectory for initial few points corresponding to the cells depicted in *A* and *B*, respectively. The first few points are marked with numbers to show that the centroid executes a random motion. Only later does the walk acquire a directionality that is indicated by a black arrow; corresponding arrows are marked in *A* and *B*.

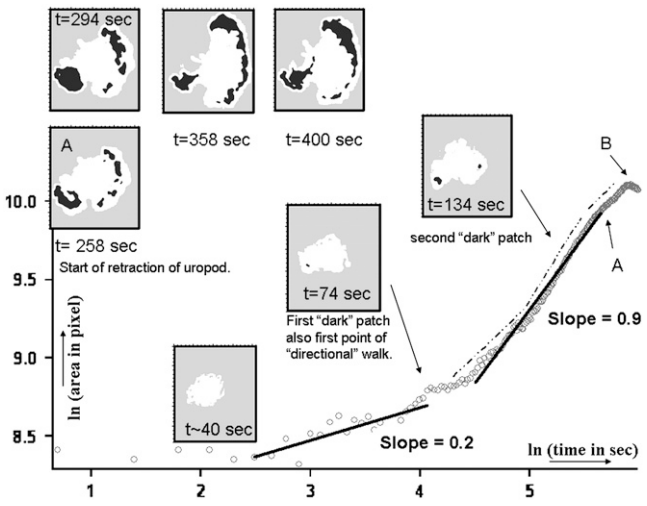

FIGURE 4 A typical area growth curve plotted as log-log plot (stimulation with a gradient of fMLF—same cell as Fig. 3 *B*). The open circles represent the data. The slow growth regime is fitted to a line (*solid*) with slope of 0.2. The fast growth regime is fitted to a single line (*solid*) of slope 0.9. Also indicated are three broken lines in the fast growth regime running next to the data points which represent piecewise fits (laterally shifted in position for clarity) with slopes 0.6, 1.0, and 0.7. The insets show trinary images of the cell corresponding to the indicated times. Note that the first change in slope marks the transition from slow to fast spreading and corresponds to the appearance of the first point of persistent close contact. The point marked *A* corresponds to the beginning of retraction of the uropod, and the point *B* marks the point at which the uropod retraction rate overtakes the lamellipod-spreading rate, resulting in a drop of the total area. (See supporting material for a similar plot along with the time-lapse images for the uniform stimulation case.)

anisotropic spreading gives rise to a directional motion of the centroid even before the cell has actually spread and started to migrate (Fig. 3, *C* and *D*). The centroid initially executes a random walk and then starts a unidirectional motion. The speed at which the centroid moves in this anisotropic stage of spreading is on the order of 0.02 μm/s, which is about one order of magnitude slower than the speed during cell migration. A logarithmic plot of the area as a function of time (Fig. 4) reveals that the spreading process can be described by power law functions fitted piecewise. The area, A, scales with time, t, as $A \sim t^b$. Distinct regimes are apparent, each with a different exponent b.

In all the cells observed, there is an initial regime of slow growth where the growth is rather irregular and the exponent b is very low $\sim$0.2 (see Fig. 5 for a statistical overview of the data). This slow spreading regime lasts for $\sim$30 s to 1 1/2 min after the first shape change of the cell. Typically, this initial stage of the spreading does not involve formation of regions of tight adhesion (close contact with substrate). The cell simply changes shape and aligns its dorsal side along the substrate. The cell membrane fluctuates near the substrate, but no nontransient and growing adhesion zones are formed. The centroid of the cell executes a random motion, but it is not clear whether this is a Brownian motion arising from the lack of attachment to the substrate or it arises because of nonuniform spreading of the cell.

The next stage corresponds to a regime of fast area growth. The exponent lies between 0.4 and 1.5. This regime of fast growth lasts typically for a few minutes. Invariably, the initiation of the fast regime corresponds to the appearance of the first area of lasting strong attachment that grows with time. The beginning of the directional walk of the centroid either exactly matches or closely follows the beginning of this regime. The polarization of the cell (defined by a visually recognizable difference between a fast spreading ''front'' and an almost stationary ''back'') happens during this regime as well. When the cells are activated by a uniform concentration of chemoattractant, where no definite gradient is present, the first direction of spreading and the first point of attachment always roughly correspond to the direction of the first steps the cells finally take (Fig. 3, *A* and *C*). In contrast,

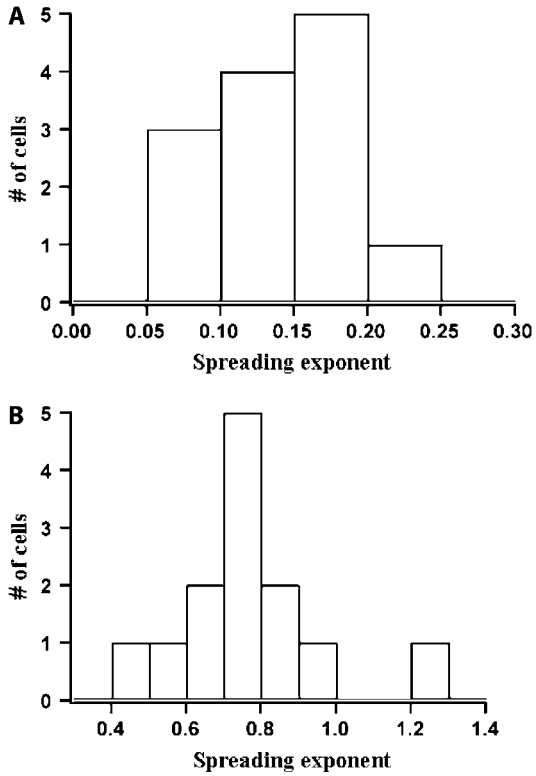

FIGURE 5 Statistical overview of the spreading exponents. (*A*) Slow spread regime. (*B*) Fast spread regime. In cases where there was more than one exponent for the fast spread regime, the different slopes were averaged.

when a gradient in the chemoattractant is present (in the case of delivery through micropipette), the first spreading and attachment is down the gradient (away from the source) and this later becomes the uropod. This regime of reverse spreading is very short lived: the cell soon reverses its direction of spreading and begins to spread toward the source, forming a well-defined, fast spreading lamellipodium (Fig. 3, *B* and *D*).

Often, this regime of fast spreading can be broken down into up to three different regimes with exponents of 0.6–0.8 for the first regime, exponents of 1–1.5 for the second regime, and exponents of 0.6–0.8 for the third regime (*dotted lines* in Fig. 4). Some cells may not display one or two of these regimes, but all cells display at least one of them (see Fig. 5 for a statistical overview of the data). In the cases when this fast regime can be further subdivided (both for uniform concentrations and gradients), the first of three regimes (exponent ~0.7) corresponds to the appearance of the first point of close contact, the second regime (exponent ~1.2) is marked by the appearance of a second point of close contact, and the third regime (exponent ~0.7) corresponds to the beginning of the withdrawal of the lamellipod. The second contact point typically appears at the opposite end of an already asymmetric cell. One of these points becomes the spreading front and the other the uropod. In the case of stimulation affected by a rise in bulk concentration of fMLF (uniform case), the first point of contact always becomes the lamellipod; but in the case of stimulation with a gradient, usually the second point of contact becomes the lamellipod. In both cases, in this fast spreading regime the principle direction of spreading is the eventual direction of migration. In the case of a gradient, this is also the direction of the applied gradient.

The areas of relatively tight adhesion are highly dynamic and not only grow but also shift their lateral position. At this stage, even though the cell is polarized in the sense that the back and the front are distinguishable in terms of their spreading rates, there is no retraction of the uropod. The cell spreads in all directions though the spreading is highly anisotropic in the sense that the front (that would become the lamellipodium) spreads much faster than the rear (that would become the uropod). The third of the fast spreading regimes corresponds to the beginning of the retraction of the uropod. However at this stage the spreading of the front, which by now is usually identifiable as a lamellipodium, continues to spread very fast, whereas the retraction of the uropod is very slow. As a result, though the growth in the area slows down, the overall increase of cell area continues. The end of the regime of fast growth is marked by a rapid retraction of the uropod. The area plateaus or begins to fall. Fig. 4 illustrates a summary of the above discussion.

Regions of close contact adhesion and their rate of growth

In addition to the total projected cell area that can be read off from the binary images, the area of tight adhesion zones can be calculated from the trinary images. Fig. 6 *A* shows a typical growth curve for regions of strong adhesions. The corresponding growth curve for the cell area is also shown in the same graph. As expected from previous discussions, the growth curve for the strong adhesion regions starts to rise sometime after the cell area starts to rise. It also saturates first (Fig. 6 *B*) and oscillates around a saturation value.

Treatment with cytochalasin-B or latrunculin-A

As in the case of untreated cells, when neutrophils treated with 2 μM cytochalasin-B are allowed to sediment, they hover over the substrate (at a distance of ~50–200 nm). When the neutrophils are subsequently activated by the addition of fMLF (no gradient), they spread to a certain extent but the area saturates very fast. The saturation area is typically ~100 μm^2. Moreover, unlike nontreated cells, they failed to develop polarity or to subsequently migrate. Fig. 7 shows the outlines of a cell treated with cytochalasin-B as it spread after activation. It can be seen that the cell spreads isotropically—there is no pinning of the kind observed for untreated cells (Fig. 3 *A*). Moreover, the trajectory of the centroid executes a random motion even at late times. All of this indicates that treatment with cytochalasin-B interferes quite severely with the structure and function of the entire actin

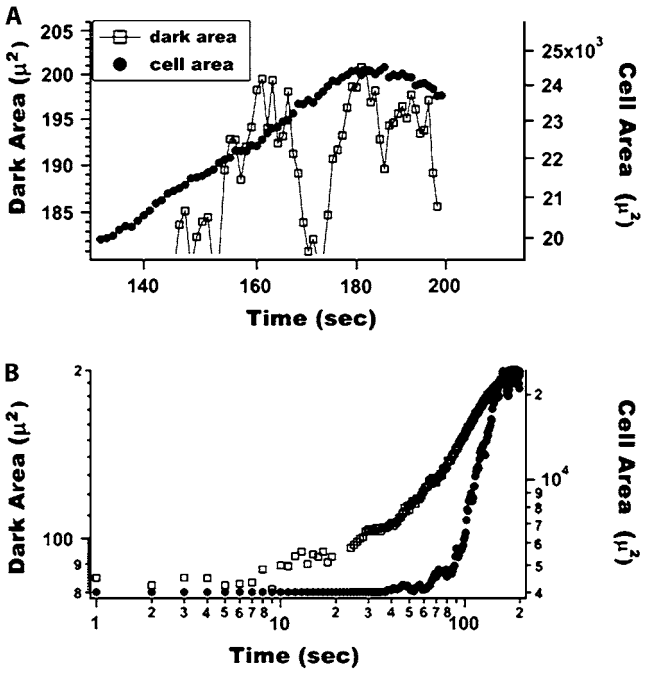

FIGURE 6 Late time oscillations (*A*) and time evolution (*B*) of cell area (*solid circles*) and adhesion area (*open squares*). (Stimulation with a gradient of fMLF—same cell as Figs. 3 *B* and 4).

cytoskeleton, resulting in altered spreading dynamics. Even though cytochalasin-B interferes with polarity and migration as well as overall spreading dynamics, the area growth curve again first grows slowly and later enters a faster growth regime.

Neutrophils treated with 2 μM latrunculin-A first sediment and hover over the substrate without spreading. Upon activation with fMLF they undergo an initial attachment to the surface; however, they fail to spread or subsequently exhibit locomotion. The cell area does not increase, but a small dark adhesion area develops. Frequently the cells bleb and expel vesicles that are then capable of adhering to the substrate. Thus, at the same concentration, latrunculin-A is more effective than cytochalasin-B in depolymerizing the actin cytoskeleton and interferes severely with the overall cell shape, resulting in a loss of the ability of the cell to spread at all.

DISCUSSION

Neutrophils are the first cells of the innate immune system to respond to a threat to the body. This response is a multistep process, where the neutrophils adhere to the endothelial wall, roll, stop (firm adhesion), spread, transmigrate through the endothelial wall, crawl to the site of infection, and phagocytose endogenous material or cell debris. Throughout these events, different chemical signaling events take place and physical forces are exerted. Some of these steps have been widely studied (e.g., rolling) both experimentally and theoretically, whereas other steps are just beginning to be explored (e.g., spreading and transmigration). In this article we study the spreading of human neutrophils on a protein-coated substrate when stimulated with a chemoattractant. We have followed the fate of the neutrophils from the initial shape changes up to the first crawling-like steps. Use of RICM and customized computer algorithms enabled us to monitor simultaneously the overall shape of the cell (including any lamellipodia) and the areas of tight adhesion.

The neutrophils initially exhibit a rounded shape and are suspended at a height of ~100–200 nm above the substrate. Upon activation by a chemoattractant, either presented as a uniform solute in the medium or as a gradient, they begin to spread; after some time they develop close contact with the substrate and finally they migrate. The spreading is anisotropic and the direction of this anisotropy presages the direction of migration. Two distinct spreading regimes are apparent, both of which can be described by a power law of the form $A \sim t^b$ where A is the spread area and t the time. The exponent b is ~0.2 for the slow spreading regime and ~0.6 for the fast spreading regime. The spreading behavior is altered by treatment with actin-depolymerizing agents like cytochalasin-B and latrunculin-A.

With regard to the substrate to membrane distance, the cell exists in two states: one corresponding to the slow spreading regime where the cell membrane is at some distance from the substrate (we estimate this distance to be between 50 and 150 nm)—the other corresponding to the fast spreading regime where the cell membrane is partially attached to the substrate (by this we mean that the cell-substrate distance is $<$50 nm for patches spanning several pixels). Such bimodal distributions have been observed in the case of dimyristoylphosphatidylcholine vesicles (doped with lipids bearing polyethylene glycol (PEG)-modified headgroups that act as repellers and mimic the glycocalyx) adhering nonspecifically to passivated glass substrates (29). In the case of the vesicles, the two states correspond to two different free energy minima that in turn correspond to the presence or absence of PEG repellers in the adhesion zone. In the case of neutrophils, two possible sources of such repulsive interaction (analog of PEG) could account for the existence of the two adhesion states: the microvilli present on the cell surface or mucins and sugars on the cell surface that make up the glycocalyx.

The cell membrane can form large patches of adhesion area only when the microvilli disappear, otherwise these small protrusions would hold the cell off the glass surface because of steric interactions. In fact, it has been observed (16) that microvilli disappear from the cell surface when cells spread. Furthermore, during rolling of neutrophils on E-selectin surfaces, the neutrophil only attaches to the surface through the microvilli (30) and the cell body of the neutrophil can barely be seen by RICM (results not shown). As soon as the neutrophil is activated with fMLF, it stops rolling and subsequently spreads and crawls on the surface. At the moment that the neutrophil stops, we believe that the microvilli start to disappear and slow spreading begins, presumably a consequence

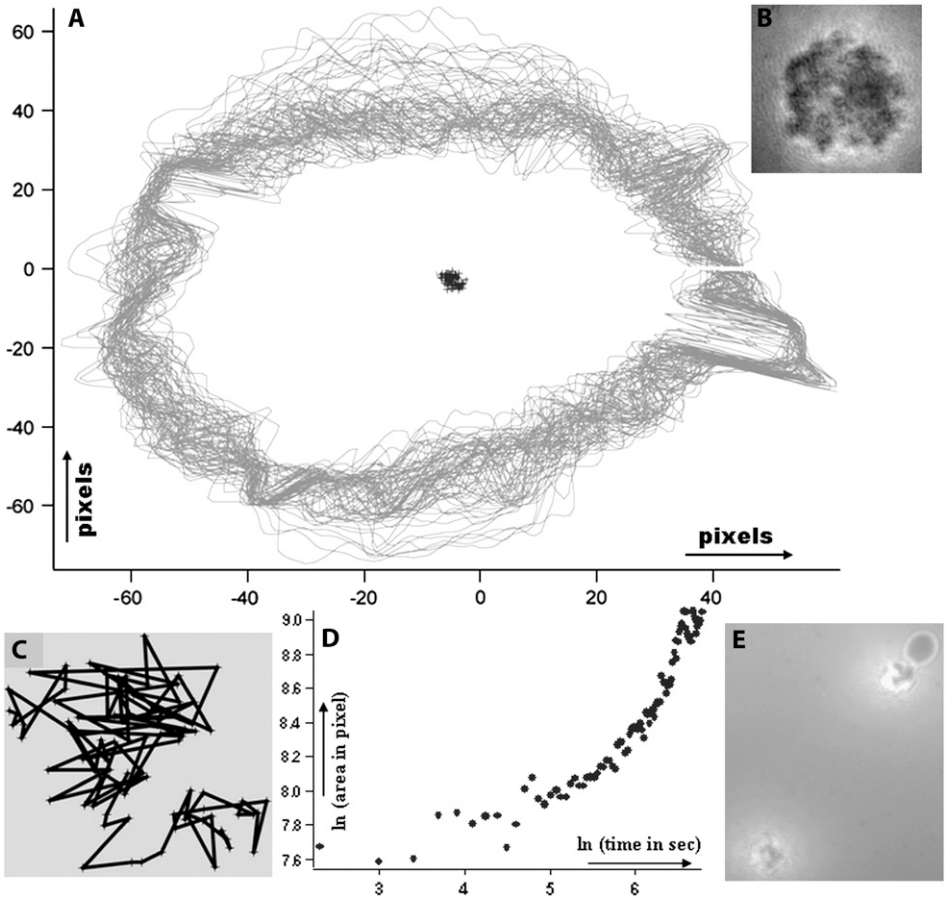

FIGURE 7 Spreading of neutrophils treated with either cytochalasin-B (*A–D*) or latrunculin-A (*E*) after activation by exposure to a uniform concentration of fMLF. (*A*) Contours describing the boundaries of a spreading cell. (*B*) RICM image. (*C*) Trajectory. (*D*) Area growth curve after treatment with cytochalasin-B. (*E*) RICM image after treatment with latrunculin-A.

of F-actin rearrangement. Treatment with cytochalasin-B is expected to decrease the density and length of microvilli on the cell surface (28,30). However, it turned out that this treatment interferes strongly with the whole actin cytoskeleton, resulting in a markedly different spreading pattern. Despite that, a slow and a fast regime are apparent (Fig. 7 *D*).

A possible role for the cell surface glycocalyx is suggested by several observations reported in the literature. The experiments of Seveou et al. (31,32) indicate that CD43, a cell-surface sialoglycoprotein and an important component of the neutrophil glycocalyx, is redistributed during spreading. Within the first minute after activation, the distribution of fluorescently labeled CD43 molecules goes from uniform to patchy. This kind of redistribution has been observed for other membrane components as well (21). Moreover, disruption of the membrane structure by extraction of cholesterol from the membrane interferes with spreading and subsequent migration (33). Recently hyaluronan, a polysaccharide consisting of glycosa-aminoglycan units which is present on the surface of most cells, has been implicated in formation of a weak adhesion preceding the well-known integrin-mediated focal adhesion formation in fibroblasts. In this case too, an initial distinct adhesion state involving a cell surface polymer (in this case hyaluronan) as well as a redistribution of the polymer is apparent (34). Thus it seems possible that the early slow phase of neutrophil spreading is associated with a redistribution of the glycocalyx.

Similar cell-spreading experiments have been reported on fibroblasts (8), macrophages (11), and amoeba (18). In the case of fibroblasts, power laws similar to those reported here were observed (35), though no possible mechanism for the different regimes was suggested. Fibroblasts have a substantial glycocalyx which may play the same role in hindering initial fast adhesion. However, in the case of macrophages where a substantial glycocalyx is also present, no such initial slow growth phase was reported (11). The present theoretical models of cell-spreading dynamics (17,18) do not accommodate the possibility of two adhesion states or two dynamical regimes.

A striking observation was that the spreading of neutrophils is anisotropic even during the initial stages of spreading. The projected cell shape deviates from a circle as the area increases. However, at this stage a single RICM image often does not reveal the underlying asymmetry, and nothing can be said about the distinction between the front and the rear (Fig. 3). However, when the time evolution of the cell profile is examined, it is revealed that after a few initial seconds, one end of the cell (destined to become the front or

the lamellipod) spreads much faster than the other (destined to become the back or the uropod). Thus a polarization of the cell is detectable even before it makes intimate contact with the substrate.

The first strong adhesion (as indicated by intimate contact with the substrate) appears not far from the edge. Careful inspection of the RICM pictures does not reveal any filopodia at this point. Later however, in addition to the tight adhesions that show up in the trinary images, there are sometimes small filopodia along the cell edge that are not recognized by our algorithm as tight adhesions. At present, we are unable to automate the recognition of the filopodia, but we have manually inspected the spreading movies and we conclude that the filopodia do not play a role in spreading. However, they may of course play a role in subsequent migration.

The appearance of the first point of tight adhesion corresponds to a transition to a fast spreading regime. In this regime, the spreading area often grows almost linearly. This kind of linear growth of the adhesion area is seen also in the case of spreading of giant unilamellar vesicles with mobile anchors in the diffusion-limited regime (25,36). However, this similarity in the exponent is likely to be a coincidence since the spreading of a cell, especially in the later stages, is expected to be an active process involving consumption of energy. Unlike vesicles, in the case of cells the zone of tight adhesion is not static—parts of the membrane that bind to the substrate do not necessarily remain bound. Even before the cell enters the phase of uropod retraction, the adhesion zones are highly mobile and often dissolve and reform. By knowing the locations of the tight adhesion zones, it is possible to argue that these zones will be where the neutrophil exert the maxima traction forces on the substrate.

We have looked at neutrophils spreading after activation on fibronectin, ICAM-1, E-selectin, and BSA as well as spontaneous spreading of neutrophils on glass (data not shown). In all cases, there is an initial slow spreading regime, a later time fast spreading regime, and finally a saturation regime. We have looked at the case of spreading after activation but with no gradient in the activating agent and also the case of spreading in an imposed gradient. The slopes and durations of the spreading regimes are similar in all cases, indicating that this kind of spreading is an intrinsic property of the cells. It turns out that the slopes are more reproducible than the durations, which seem to depend strongly on the individual donor. Neutrophils from the same donor exhibit similar spreading times, but this time varies by up to ~100% from donor to donor.

The instantaneous velocities of the cell-membrane segments can be computed from our analysis and are found to be random. The cell spreads by many small steps of the membrane, which can be either outwards or inwards at any given moment. Whether in the long term there is spreading or not is determined by the relative numbers of forward and backward steps. In an earlier publication, Dubin-Thaler et al. (8) reported that spreading of fibroblasts is characterized by a periodic retraction regime at late times. No such periodicity was observed in the case of neutrophils, perhaps because the observed effects occur at a shorter timescale than we observed.

Treatment of the cells with cytochalasin-B (concentration, 2 μM), which is an actin-depolymerizing agent that caps the growing end of polymerizing f-actin filaments, did not affect the presence of the different spreading regimes. It however eliminated the polarization of the cell (as judged from spreading profiles as described above; compare Figs. 3 and 7). Interestingly, when the cell is treated in this way, the final spreading area for all the cells saturates to ~100–200 μm^2. In contrast, untreated cells exhibit widely varying saturation area. In the absence of active contributions coming from actin polymerization, the saturation area in the case of cytochalasin-B-treated cells is likely to be determined by a balance between adhesive forces and membrane tension. In fact, treating the cells as vesicles with no area or volume constraint and assuming that cytochalasin-B treatment does not change the relevant surface tension, it can be estimated that there are ~100 bonds/μm^2. This is in qualitative agreement with the value of 500 bonds/μm^2 reported in Frisch and Thoumine (17).

Latrunculin-A inhibits the polymerization of actin by recruiting actin monomers, and it has been reported that latrunculin-A is actively sequestered by neutrophils thus

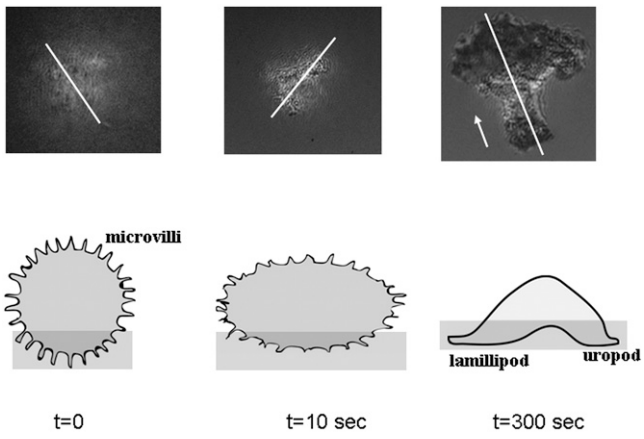

FIGURE 8 (*Top row*) Raw RICM images of neutrophils at three different spreading states. (*Bottom row*) Inferred shapes of the neutrophil—side view along the corresponding white line (not to scale since the microvilli should be ~1000 times smaller than the cell body; the presence of the microvilli is supposed and not directly detected by RICM; the *light gray rectangles* indicate the depth to which RICM can probe). A model for neutrophil spreading can be constructed based on these diagrams. Initially, the cell is held at height h ($\sim 200 > h > \sim 100$ nm) by balance between gravity and steric repulsion due to microvilli (~100–300 nm long) and/or the glycocalyx (~200 nm thick). After activation the cell starts changing its shape, and presumably the microvilli (and the glycocalyx) start disappearing. There is still no intimate contact with the substrate because of the presence of microvilli and/or the glycocalyx ($\sim 100 > h > 50$ nm); the cell is in the slow spread regime. Finally, the microvilli (and/or the glycocalyx) disappear and the cell starts adhering ($h < \sim 50$ nm). Zones of intimate contact (''tight adhesion'') appear, and the cell enters the fast spread regime.

increasing the efficiency of depolymerization (37). In this case, treatment with latrunculin-A (concentration, 2 μM) completely prevents the cells from spreading. However, upon activation the cells still undergo an initial adhesion (Fig. 7 *E*), showing that the adhesive molecules remain active even after latrunculin-A treatment and do not need an intact actin cytoskeleton to participate in binding.

In summary, from our results on the spreading of neutrophils a model for initial neutrophil motility during chemokinesis as well as chemotaxis follows (Fig. 8): First, the neutrophil spreads slowly, without forming intimate contact with the substrate, getting rid of microvilli and/or glycocalyx. At this stage the neutrophil already shows a polarity as judged by the spreading dynamics. Next, an initial spot of more intimate contact with the substrate is formed that can later become either the lamellipod or uropod. The neutrophil enters a stage of fast spread on the substrate. Soon, another adhesion spot appears at the opposite pole of the neutrophil, which becomes the uropod (or lamellipod depending on the fate of the first spot of intimate contact). At this point, the neutrophil is still in the fast spreading regime. Afterwards, the spreading area saturates and crawling begins. Thus, initiation of intimate contact with the substrate may be involved in the determination of neutrophil polarity.

K.S. thanks L. Limozin for extensive discussions on image processing and P. Bongrand for discussions on cell spreading.

P.J., D.H., and K.S. acknowledge financial support from National Institutes of Health (NIH) grant HL64388 and National Science Foundation/Materials Research Science and Engineering Centers DMR05-20020. D.H. acknowledges support from NIH HL18208.

REFERENCES

1. Lipowsky, H. H. 1995. Leukocyte margination and deformation in postcapillary venules. *In* Physiology and Pathophysiology of Leukocyte Adhesion. D. N. Granger and G. W. Schmid-Schönbein, editors. Oxford University Press, New York. 130–147.
2. Sanchez-Madrid, F., and M. A. del Pozo. 1999. Leukocyte polarization in cell migration and immune interactions. *EMBO J.* 18:501–511.
3. Alon, R., D. A. Hammer, and T. A. Springer. 1995. Lifetime of the P-selectin-carbohydrate bond and its response to tensile force in hydrodynamic flow. *Nature.* 374:539–542.
4. Simon, S. I., and C. E. Green. 2005. Molecular mechanics and dynamics of leukocyte recruitment during inflammation. *Annu. Rev. Biomed. Eng.* 7:151–185.
5. Ramachandran, V., M. Williams, T. Yago, D. W. Schmidtke, and R. P. McEver. 2004. Dynamic alterations of membrane tethers stabilize leukocyte rolling on P-selectin. *Proc. Natl. Acad. Sci. USA.* 101: 13519–13524.
6. Laudanna, C., J. Y. Kim, G. Constantin, and E. Butcher. 2002. Rapid leukocyte integrin activation by chemokines. *Immunol. Rev.* 186:37–46.
7. Yang, L., R. M. Froio, T. E. Sciuto, A. M. Dvorak, R. Alon, and F. W. Luscinskas. 2005. ICAM-1 regulates neutrophil adhesion and transcellular migration of TNF-alpha-activated vascular endothelium under flow. *Blood.* 106:584–592.
8. Dubin-Thaler, B. J., G. Giannone, H. G. Dobereiner, and M. P. Sheetz. 2004. Nanometer analysis of cell spreading on matrix-coated surfaces reveals two distinct cell states and STEPs. *Biophys. J.* 86:1794–1806.
9. Reinhart-King, C. A., M. Dembo, and D. A. Hammer. 2005. The dynamics and mechanics of endothelial cell spreading. *Biophys. J.* 89:676–689.
10. Zicha, D., I. M. Dobbie, M. R. Holt, J. Monypenny, D. Y. Soong, C. Gray, and G. A. Dunn. 2003. Rapid actin transport during cell protrusion. *Science.* 300:142–145.
11. Pierres, A., P. Eymeric, E. Baloche, D. Touchard, A. M. Benoliel, and P. Bongrand. 2003. Cell membrane alignment along adhesive surfaces: contribution of active and passive cell processes. *Biophys. J.* 84:2058–2070.
12. Hategan, A., K. Sengupta, S. Kahn, E. Sackmann, and D. E. Discher. 2004. Topographical pattern dynamics in passive adhesion of cell membranes. *Biophys. J.* 87:3547–3560.
13. Sackmann, E., and R. F. Bruinsma. 2002. Cell adhesion as wetting transition? *ChemPhysChem.* 3:262–269.
14. Bell, G. I., M. Dembo, and P. Bongrand. 1984. Cell adhesion. Competition between nonspecific repulsion and specific bonding. *Biophys. J.* 45:1051–1064.
15. Bell, G. I. 1978. Models for the specific adhesion of cells to cells. *Science.* 200:618–627.
16. Pierre, A., A. Benoliel, and P. Bongrand. 2000. Cell-cell interaction. *In* Physical Chemistry of Biological Interfaces. A. Baszkin and W. Norde, editors. Marcel Dekker, New York. 459–522.
17. Frisch, T., and O. Thoumine. 2002. Predicting the kinetics of cell spreading. *J. Biomech.* 35:1137–1141.
18. Chamaraux, F., S. Fache, F. Bruckert, and B. Fourcade. 2005. Kinetics of cell spreading. *Phys. Rev. Lett.* 94:158102.
19. Wilkinson, P. C. 1986. The locomotor capacity of human lymphocytes and its enhancement by cell growth. *Immunology.* 57:281–289.
20. Zigmond, S. H., H. I. Levitsky, and B. J. Kreel. 1981. Cell polarity: an examination of its behavioral expression and its consequences for polymorphonuclear leukocyte chemotaxis. *J. Cell Biol.* 89: 585–592.
21. Pierini, L. M., R. J. Eddy, M. Fuortes, S. Seveau, C. Casulo, and F. R. Maxfield. 2003. Membrane lipid organization is critical for human neutrophil polarization. *J. Biol. Chem.* 278:10831–10841.
22. Cicchetti, G., P. G. Allen, and M. Glogauer. 2002. Chemotactic signaling pathways in neutrophils: from receptor to actin assembly. *Crit. Rev. Oral Biol. Med.* 13:220–228.
23. Xu, J., F. Wang, A. Van Keymeulen, P. Herzmark, A. Straight, K. Kelly, Y. Takuwa, N. Sugimoto, T. Mitchison, and H. R. Bourne. 2003. Divergent signals and cytoskeletal assemblies regulate self-organizing polarity in neutrophils. *Cell.* 114:201–214.
24. Servant, G., O. D. Weiner, P. Herzmark, T. Balla, J. W. Sedat, and H. R. Bourne. 2000. Polarization of chemoattractant receptor signaling during neutrophil chemotaxis. *Science.* 287:1037–1040.
25. Kloboucek, A., A. Behrisch, J. Faix, and E. Sackmann. 1999. Adhesion-induced receptor segregation and adhesion plaque formation: a model membrane study. *Biophys. J.* 77:2311–2328.
26. Curtis, A. S. G. 1964. The mechanism of adhesion of cells to glass. A study by interference reflection microscopy. *J. Cell Biol.* 20: 199–215.
27. Riveline, D., E. Zamir, N. Q. Balaban, U. S. Schwarz, T. Ishizaki, S. Narumiya, Z. Kam, B. Geiger, and A. D. Bershadsky. 2001. Focal contacts as mechanosensors: externally applied local mechanical force induces growth of focal contacts by an mDia1-dependent and ROCK-independent mechanism. *J. Cell Biol.* 153:1175–1186.
28. Finger, E. B., R. E. Bruehl, D. F. Bainton, and T. A. Springer. 1996. A differential role for cell shape in neutrophil tethering and rolling on endothelial selectins under flow. *J. Immunol.* 157:5085–5096.
29. Marx, S., J. Schilling, E. Sackmann, and R. Bruinsma. 2002. Helfrich repulsion and dynamical phase separation of multicomponent lipid bilayers. *Phys. Rev. Lett.* 88:138102.
30. Schmidtke, D. W., and S. L. Diamond. 2000. Direct observation of membrane tethers formed during neutrophil attachment to platelets or P-selectin under physiological flow. *J. Cell Biol.* 149:719–730.

31. Seveau, S., H. Keller, F. R. Maxfield, F. Piller, and L. Halbwachs-Mecarelli. 2000. Neutrophil polarity and locomotion are associated with surface redistribution of leukosialin (CD43), an antiadhesive membrane molecule. *Blood*. 95:2462–2470.

32. Dehghani Zadeh, A., S. Seveau, L. Halbwachs-Mecarelli, and H. U. Keller. 2003. Chemotactically-induced redistribution of CD43 as related to polarity and locomotion of human polymorphonuclear leucocytes. *Biol. Cell*. 95:265–273.

33. Tian, W., I. Laffafian, S. Dewitt, and M. B. Hallett. 2003. Exclusion of exogenous phosphatidylinositol-3,4,5-trisphosphate from neutrophil-polarizing pseudopodia: stabilization of the uropod and cell polarity. *EMBO Rep*. 4:982–988.

34. Cohen, M., Z. Kam, L. Addadi, and B. Geiger. 2006. Dynamic study of the transition from hyaluronan- to integrin-mediated adhesion in chondrocytes. *EMBO J*. 25:302–311.

35. Dobereiner, H. G., B. Dubin-Thaler, G. Giannone, H. S. Xenias, and M. P. Sheetz. 2004. Dynamic phase transitions in cell spreading. *Phys. Rev. Lett*. 93:108105.

36. Cuvelier, D., and P. Nassoy. 2004. Hidden dynamics of vesicle adhesion induced by specific stickers. *Phys. Rev. Lett*. 93:228101.

37. Pring, M., L. Cassimeris, and S. H. Zigmond. 2002. An unexplained sequestration of latrunculin A is required in neutrophils for inhibition of actin polymerization. *Cell Motil. Cytoskeleton*. 52: 122–130.